Доклади на Българската академия на науките
Comptes rendus de l'Académie bulgare des Sciences
Tome 78, No 3, 2025

ENGINEERING SCIENCES
Control theory

PATH FOLLOWING CONTROL OF BI-STEERABLE CARS: A LYAPUNOV-BASED APPROACH

Plamen Petrov[1]✉, Ivan Kralov[2]

Received on November 8, 2024
Presented by Ch. Roumenin, Member of BAS, on January 28, 2025

Abstract

Path following control is important in order to realize autonomous driving of robotic vehicles. The need to move automated cars in cluttered environments, as well as parking in tight places, often leads to following complex reference paths with small radius of curvature, which can be implemented successfully by vehicles with increased manoeuvrability, such as the four-wheel steering (4WS) cars. This paper proposes a feedback path control law for a bi-steerable car (4WS vehicle where the steering angle of the rear wheels is a function of the steering angle of the front one). First, kinematic model of the car in error coordinates expressed in a moving reference frame, which is partially linked to the vehicle is derived. The control law is constructed using Lyapunov-based control design techniques, yielding asymptotic stability of the closed-loop system in error coordinates. Simulation results illustrate the effectiveness of the proposed controller.

Key words: bi-steerable car, kinematic model, path following, Lyapunov-based control design

1. Introduction. The control of automated vehicles has been subject of research interest for more than two decades [1–4]. Path following is one of the basic

This research was funded by the European Regional Development Fund within the Operational Programme "Bulgarian national recovery and resilience plan", procedure for direct provision of grants "Establishing of a network of research higher education institutions in Bulgaria", and under Project BG-RRP-2.004-0005, "Improving the research capacity anD quality to achieve intErnAtional recognition and reSilience" of TU-Sofia (IDEAS).

https://doi.org/10.7546/CRABS.2025.03.13

tasks, which has to be fulfilled in order to achieve vehicle's autonomous driving capability [5]. The nonlinear behaviour and nonholonomic nature of the vehicles render the path following control a challenging task. The need to move automated cars in cluttered environments, as well as parking in tight places, poses challenges to perform manoeuvres in a confined space and achieve a path with a smaller turning radius. In order to obtain enhanced manoeuvrability, one solution which becomes increasingly relevant is a car with four steering wheels [6]. In recent years, there has been considerable effort in the development of tracking controllers for automated vehicles with four steering wheels (4WS), which possess the ability to steer both the front and the rear wheels. A particular type of 4WS vehicles is the so-called "bi-steerable" car, which is designed such that the front and rear wheels are steered opposite to each other, so that the steering angle of the rear wheels is a function of the steering angle of the front wheels [7]. The capability to steer both front and rear wheels (double steering mode) achieves small turning radius and increases the car manoeuvrability, and is employed mainly at low speed manoeuvres. Several control strategies have been reported in the literature for path following of bi-steerable vehicles, including sliding mode [8] and geometrical pure pursuit tracking method [9]. In this paper, we propose a path following controller for a bi-steerable car. The path following error kinematics is derived with respect to a reference coordinate system attached to the reference path. The control law is constructed using a Lyapunov-oriented control design technique. Asymptotic stability of the closed-loop subsystem for the car lateral and orientation errors is achieved. Simulation results are presented in order to illustrate the effectiveness of the proposed controller.

2. Bi-steerable car model and problem formulation. ***2.1. Bi-steerable car kinematic model.*** A schematic illustration of the bi-steerable vehicle geometry in the plane is shown in Fig. 1. To simplify the derivation of the kinematic vehicle kinematic model, we use a planar bicycle car model, where two virtual wheels are located at the mid-points of the car's front and rear wheel axles (Fig. 1). It is assumed that they comply with the condition of pure rolling without slipping.

In order to describe the position and the orientation of the car in the plane, the following coordinate systems are assigned (Fig. 1): Fxy – inertial (global) coordinate system in the plane of motion; Sxy and Pxy – body-fixed coordinate systems with centres placed at the mid-points of the front and rear car axles; W_1xy and W_2xy – wheel coordinate systems with centres placed at the mid-points of the front and rear car axles and oriented in the direction of the front and rear virtual wheels, respectively; Rx_ry_r – moving reference coordinate system, partially linked to the car, such that the x_r axis is tangent to the reference path and orinted in the direction to follow, and the y_r axis passes through the reference point S of the car.

Throughout this paper, the following notations are used:

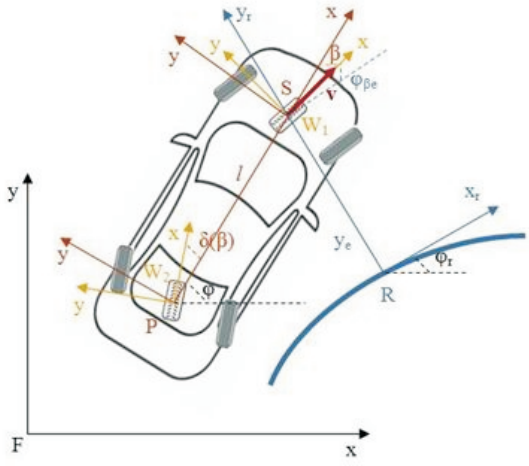

Fig. 1. Schematic diagram of the bi-steerable car in the plane and the corresponding bicycle model

- ${}^{F}r_H = \begin{bmatrix} x_H \\ y_H \end{bmatrix} \in R^2$ indicates the position vector of the coordinates of a point H with respect to the global coordinate system Fxy;
- ${}^{F}v_H = \begin{bmatrix} \dot{x}_H \\ \dot{y}_H \end{bmatrix} \in R^2$ indicates the velocity vector of a point H with respect to the global coordinate system Fxy;
- ${}^{G}v_H = \begin{bmatrix} {}^{G}v_{Hx} \\ {}^{G}v_{Hy} \end{bmatrix} \in R^2$ indicates the velocity vector of a point H with respect to the global coordinate system Fxy expressed in a body-fixed coordinate system Hxy;
- ${}^{G}R_H(\theta) = \begin{bmatrix} \cos\theta & -\sin\theta \\ \sin\theta & \cos\theta \end{bmatrix} \in SO(2)$ represents an orthogonal rotation matrix of angle θ, where H and G stand for the beginning and destination coordinate frames, respectively;
- $S(\omega_H) = \begin{bmatrix} 0 & -\omega_H \\ \omega_H & 0 \end{bmatrix} \in SS(2)$ represents a skew-symmetric matrix, where ω_H is the angular velocity of a rotating frame Hxy with respect to the global coordinate system Fxy.

The following parameters and variables of the car and the reference path are defined as follows: l is the distance between the front and rear wheel axles; φ is the orientation of the car with respect to Fxy; β, $\delta(\beta)$ is the orientation of the front

and rear virtual steering wheels with respect to body-fixed coordinate frames Sxy and Pxy, respectively; φ_r is the orientation of the reference coordinate system Rx_ry_r with respect to Fxy.

In the inertial frame Fxy, the system configuration can be described by the following generalized coordinates

$$q = [x_s, y_s, \varphi, \beta]^T \in R^4. \tag{1}$$

The kinematic nonholonomic constraints arising from the pure rolling without slipping condition of the front and rear car wheels, can be expressed in local wheel-fixed coordinate frames W_1xy and W_2xy, as follows

$$^{W_1}v_{W_1y} = 0; \qquad ^{W_2}v_{W_2y} = 0. \tag{2}$$

In order to obtain expressions of the nonholonomic constraints, in terms of the generalized velocities $\dot{q} = [\dot{x}_S, \dot{y}_S, \dot{\varphi}, \dot{\beta}]^T$, the velocity of points W_1 and W_2 relative to the inertial coordinate system Fxy and expressed in frames W_1xy and W_2xy, respectively, are sequentially determined. First, it should be noted that, since the centres of the coordinate systems Sxy and W_1xy coincide, the velocities of points S and W_1 are the same, i.e., $^Sv_S = {}^Sv_{W_1}$. Rotation matrices $^SR_{W_1}(\beta) \in SO(2)$ and $^FR_S(\varphi) \in SO(2)$ are used to obtain relationships between the components of the velocity of point W_1 and S in coordinate systems Sxy and Fxy as

$$^Sv_{W_1} = {}^SR_{W_1}(\beta)^{W_1}v_{W_1}; \qquad ^Fv_S = {}^FR_S(\varphi)^Sv_S. \tag{3}$$

Using (3), we obtain expressions for the components of the velocity of point W_1 expressed in the frame W_1xy, as follows

$$\begin{aligned} ^{W_1}v_{W_1} &= {}^SR^{-1}_{W_1}(\beta)^FR^-_S(\varphi)^Fv_S \\ &= \begin{bmatrix} \dot{x}_S\cos(\varphi+\beta) + \dot{y}_S\sin(\varphi+\beta) \\ -\dot{x}_S\sin(\varphi+\beta) + \dot{y}_S\cos(\varphi+\beta) \end{bmatrix}. \end{aligned} \tag{4}$$

With respect to the rear virtual steering wheel, it should be also noted that, since the centres of the coordinate systems Pxy and W_2xy coincide, the velocities of points P and W_2 are the same, i.e., $^Pv_P = {}^Pv_{W_2}$. Furthermore, $^Sv_P = {}^Pv_P$, because the body-fixed frames Sxy and Pxy are stationary relative to each other and have mutually parallel axes (Fig. 1). The following expression, as well as rotation matrices $^PR_{W_2}(\delta(\beta)) \in SO(2)$ and $^FR_S(\varphi) \in SO(2)$ are used to obtain relationships between the components of the velocity of point W_2 and P in coordinate systems Pxy and Fxy

$$\begin{aligned} ^Sv_P &= {}^Sv_S + \ S(\omega_S)^Sl \\ ^Pv_{W_2} &= {}^PR_{W_2}(\delta(\beta))^{W_2}v_{W_2}; \qquad ^Fv_P = {}^FR_P(\varphi)^Pv_P{}' \ , \end{aligned} \tag{5}$$

where ${}^{S}l = [-l\ 0]^T \in R^2$ and ω_S is the angular velocity of the car with respect to inertial frame Fxy.

Using (5), we obtain expressions for the components of the velocity of point W_2 expressed in the frame W_2xy, as follows

$$
\begin{aligned}
{}^{W_2}v_{W_2} &= {}^{P}R_{W_2}^{-1}(\delta(\beta))[{}^{F}R_{S}^{-1\,F}v_S + S(\omega_S)^{S}l \\
&= \begin{bmatrix} \dot{x}_S\cos(\varphi+\delta(\beta)) + \dot{y}_S\sin(\varphi+\delta(\beta)) - l\dot{\varphi}\sin(\delta 9\beta)) \\ -\dot{x}_S\sin(\varphi+\delta(\beta)) + \dot{y}_S\cos(\varphi+\delta(\beta)) - l\dot{\varphi}\cos(\delta 9\beta)) \end{bmatrix}.
\end{aligned} \tag{6}
$$

The two nonholonomic constraints (2) are obtained from the fact that the wheels move without lateral sliding in lateral direction. They are derived from the y-component of ${}^{W_1}v_{W_1}$ and ${}^{W_2}v_{W_2}$ in (4) and (6), respectively, which are equal to zero. The constraints on the generalized velocities $\dot{q}$ can be written in matrix form as

$$
N(q)\dot{q} = 0, \tag{7}
$$

where

$$
N(q) = \begin{bmatrix} -\sin(\varphi+\beta) & \cos(\varphi+\ \beta) & 0 & 0 \\ -\sin(\varphi+\delta(\beta)) & \cos(\varphi+\delta(\beta)) & -l\dot{\varphi}\cos(\delta(\beta)) & 0 \end{bmatrix} \in R^{2\times 4}. \tag{8}
$$

The car has two degrees-of-freedom in the plane. The system (7) can be converted in an affine driftless control system

$$
\dot{q} = C(q)\varsigma, \tag{9}
$$

where

$$
C = \begin{bmatrix} \cos(\varphi+\beta) & 0 \\ \sin(\varphi+\beta) & 0 \\ \dfrac{\sin(\varphi-\delta(\beta))}{\cos(\delta(\beta))} & 0 \\ 0 & 1 \end{bmatrix}, \tag{10}
$$

and

$$
\varsigma = \begin{bmatrix} v \\ \omega \end{bmatrix} \in R^{2\times 1} \tag{11}
$$

is a vector of independent quisi-velocities, where $v = {}^{W_1}v_{W_1x}$ and $\omega = \dot{\beta}$ denote the linear and angular steering velocities of the front steering wheel.

We define a new variable $\varphi_\beta \stackrel{\text{def}}{=} \varphi + \beta$. In the new coordinate variable, the system (9) is obtained in the form

$$\dot{q}_\beta = C_\beta(q_\beta)\varsigma, \tag{12}$$

where

$$C_\beta(q_\beta) = \begin{bmatrix} \cos\varphi_\beta & 0 \\ \sin\varphi_\beta & 0 \\ \dfrac{\sin(\varphi - \delta(\beta))}{\cos(\delta(\beta))} & 0 \\ 0 & 1 \end{bmatrix}, \tag{13}$$

and $q_\beta = [x_s, y_s, \varphi_\beta, \beta]^T \in R^4$.

2.2. Problem formulation. The path following geometry used in this paper is presented in Fig. 1. A reference coordinate frame Rx_ry_r is defined such that the x_r axis is tangent to the path and oriented in the direction of motion to follow. The y_r axis passes through the reference point S of the car. It is supposed that the distance between the points S and R is smaller than the reference curvature radius ρ_r in point R, which ensures that the reference frame Rx_ry_r is uniquely defined.

The coordinates and orientation of the car in the reference coordinate frame Rx_ry_r are [10, 11]

$$\begin{bmatrix} x_e \\ y_e \\ \varphi_{\beta e} \end{bmatrix} = \begin{bmatrix} \cos\varphi_r & \sin\varphi_r & 0 \\ -\sin\varphi_r & \cos\varphi_r & 0 \\ 0 & 0 & 1 \end{bmatrix} \begin{bmatrix} x_s - x_r \\ y_s - y_r \\ \varphi_\beta - \varphi_r \end{bmatrix}. \tag{14}$$

Differentiating (14) and taking into account the nonholonomic constraints (2), after some work, the error kinematics of the car is obtained in the form

$$\begin{aligned} \dot{x}_e &= -v_r + v\cos\varphi_{\beta e} + \omega_r y_e \\ \dot{y}_e &= v\sin\varphi_{\beta e} \\ \dot{\varphi}_{\beta e} &= -\omega_r + \omega_\beta \end{aligned}, \tag{15}$$

where $\omega_r = \dot{\varphi}_r$, $\omega_\beta = \dot{\varphi}_\beta$, and v_r is the velocity of the centre R of the reference frame Rx_ry_r.

It is assumed that the car velocity v is bounded and does not converge to zero, i.e., $0 < v \leq v_{\max}$. Since the reference frame Rx_ry_r is partially linked to the car (the y_r passes through the reference point S of the car), from the first equation of (15) it follows that $x_e = \dot{x}_e \equiv 0$, and using the relationship $\omega_r = \dfrac{v_r}{\rho_r} = v_r c_r$, where ρ_r and c_r are the curvature radius and the curvature of the reference path

at point R, respectively, the following relationships are obtained for the linear and angular velocity of the reference frame, as follows

$$v_r = v\frac{\cos\varphi_{\beta e}}{1 - c_r y_e}, \tag{16}$$

$$\omega_r = v\frac{c_r\cos\varphi_{\beta e}}{1 - c_r y_e}. \tag{17}$$

Finally, using (15), (16), (17) and the last two equations of (12), the error kinematics for path following applications is derived in the form

$$\begin{aligned} \dot{y}_e &= v\ \sin\varphi_{\beta e} \\ \dot{\varphi}_{\beta e} &= -v\frac{c_r\cos\varphi_{\beta e}}{1 - c_r y_e} + v\frac{\sin(\beta - \delta(\beta))}{l\cos(\delta(\beta))} + \omega \\ \dot{\beta} &= \omega \end{aligned}. \tag{18}$$

In this case, using the parameterization $(y_e, \varphi_{\beta e})$ and given a reference path, the path following problem consists of finding a feedback control $\omega = f(v, y_e, \varphi_{\beta e}, c_r)$ for the first two equations of system (18), such that

$$\begin{aligned} &\lim_{t\to\infty} y_e(t) = 0 \\ &\lim_{t\to\infty} \varphi_{\beta e}(t) = 0 \end{aligned}. \tag{19}$$

3. Control design and stability analysis. ***3.1. Lyapunov-based path control design.*** In this section, we present a feedback path following controller for a bi-steerable car, described by (18). We propose a control law design based on a reduced-order model consisting of the first two equations of (18) rewritten bellow for the clarity of exposition, i.e.

$$\begin{aligned} \dot{y}_e &= v\sin\varphi_{\beta e} \\ \dot{\varphi}_{\beta e} &= -v\frac{c_r\cos\varphi_{\beta e}}{1 - c_r y_e} + \frac{\sin(\varphi - \delta(\beta))}{\cos(\delta(\beta))} + \omega \end{aligned}. \tag{20}$$

The control objective is to regulate the state $(y_e, \varphi_{\beta e})$ to zero. To facilitate the subsequent control design, we consider the following change of coordinates

$$\begin{aligned} z_1 &= y_e \\ z_2 &= \sin\varphi_{\beta e} \end{aligned}. \tag{21}$$

We also define a new input variable

$$w = \left(-v\frac{c_r\cos\varphi_{\beta e}}{1 - c_r y_e} + v\frac{\sin(\varphi - \delta(\beta))}{l\cos(\delta(\beta))} + \omega\right)\cos\varphi_{\beta e}. \tag{22}$$

The advantage of this transformation is that it easily leads to Lyapunov control design. In the new coordinates (21) and input (22), the system (20) takes the form

$$\begin{array}{l} \dot{z}_1 = v z_2 \\ \dot{z}_2 = w \end{array} . \tag{23}$$

We chose the following Lyapunov function candidate

$$W = \frac{1}{2} z_1^2 + \frac{1}{2} (k_1 z_1 + z_2)^2, \tag{24}$$

where k_1 is a positive gain. The derivative of (24) is obtained in the form

$$\dot{W} = v z_1 z_2 + (k_1 z_1 + z_2)(k_1 v z_1 + w). \tag{25}$$

By choosing the control input w in the form

$$w = -k_1 v z_2 - v z_1 - k_2 v (k_1 z_1 + z_2), \tag{26}$$

where k_2 is a positive gain, we obtain the derivative of W as follows

$$\dot{W} = -v k_1 z_1^2 - k_2 v (k_1 z_1 + z_2)^2 < 0. \tag{27}$$

The resulting closed-loop system is obtained in the form

$$\begin{array}{l} \dot{z}_1 = v z_2 \\ \dot{z}_2 = -v(1 + k_1 k_2) z_1 - v(k_1 + k_2) z_2 \end{array} . \tag{28}$$

3.2. Stability analysis. The proof of the stability of the closed-loop system (28) is based on Lyapunov-like analysis. We now summarize our stability result in the following Proposition.

Proposition 1. *Assume that the car velocity $v(t)$ and its derivative $\dot{v}$ are bounded differentiable functions, and v does not tend to zero as $t \to \infty$, then the control* (26) *asymptotically stabilizes the system* (23).

Proof. The function (24) is positive-definite radially unbounded and its time derivative (27) along the trajectories of (28) is negative definite. Therefore, V is non-increasing ($W(t) \leq W(0)$), and this in turn implies, that $z_1(t)$ and $z_1(t)$ are bounded. Since $v(t)$ is bounded continuous function, and its derivative is bounded, $v(t)$ is uniformly continuous. Thus, $\dot{W}$ is uniformly continuous ($W(t)$ is lower-bounded), since its derivative is bounded, and by application of Barbalat's Lemma [12], it follows, that $\dot{W}(t) \to 0$ as $t \to \infty$. From the expression for $\dot{W}$ (27), it follows that $v z_1(t) \to 0$ and $v(k_1 z_1(t) + z_2(t)) \to 0$, as $t \to \infty$. In view of the last expression, since $z_1(t) \to 0$, it follows that $z_2(t) \to 0$, as $t \to \infty$. From the first equation of (28), it follows that $\dot{z}_1(t) \to 0$, as $t \to \infty$, since $z_2(t) \to 0$ and $v(t)$ does not tend to zero. From the second equation of (28), it follows that

$\dot{z}_2(t) \to 0$, as $t \to \infty$, since $z_1(t) \to 0$ and $z_2(t) \to 0$, and $v(t)$ does not tend to zero. This completes the proof. □

It should be noted that from (26), it follows that the control w is bounded, since $v(t)$, $z_1(t)$ and $z_2(t)$ are bounded.

The next step in the stability analysis is to establish that β is bounded. Defining $z_3 = \beta$, and the same control (26) designed for the second-order error dynamics (23) is applied to the third equation of (18), leads to the first-order internal dynamics given by

$$\dot{z}_3 = \frac{-k_1 v z_2 - v z_1 - k_2 v(k_1 z_1 + z_2)}{\cos(\arcsin z_2)} + v\frac{x_r \cos\varphi_{\beta e}}{1 - c_r z_1} - v\frac{\sin(\beta - \delta(\beta))}{l\cos(\delta(\beta))}. \tag{29}$$

To study the stability of the internal dynamics of the closed-loop system, we analyse the so-called zero dynamics of z_3. The zero dynamics is defined as $\dot{z}_3 = f(z_1, z_2, z_3) = f(0, 0, z_3)$. Provided that this dynamics is asymptotically stable, the proposed control will stabilize the overall closed-loop system (28). Letting $z_1(t) \equiv 0$ in (29) and $z_3(t) \neq 0$, the following equation for the zero dynamics is obtained

$$\dot{\beta} = v c_r - v\frac{\sin(\beta - \delta(\beta))}{l\cos(\delta(\beta))}. \tag{30}$$

For brevity of exposition, we will provide stability analysis in a particular case, when the car follows a rectilinear path ($c_r = 0$) with constant velocity $v = v_c = cte$. We also specify $\delta(\beta) = -k\beta$, $0 < k \leq 1$, where k is the rear-to-front steering angle ratio. In this case equation (30) for the zero dynamics takes the form

$$\dot{\beta} = -v_c\frac{\sin(\beta + k\beta)}{l\cos(\delta(\beta))}. \tag{31}$$

Proposition 2. *Consider the dynamics* (31) *and assume that for all* $t \geq 0$, $0 < v_c$ *and* $0 < k \leq 1$, *then the zero dynamics of* $z_3 \triangleq \beta$ *is asymptotically stable.*

Proof. Consider a Lyapunov function candidate

$$V = 1 - \cos(k\beta). \tag{32}$$

The derivative of (32) along the solutions of (31) is

$$\begin{aligned} \dot{V} &= -\frac{k v_c}{l}\frac{\sin(k\beta)\sin[(k+1)\beta]}{\cos(k\beta)} \\ &= -\frac{k v_c}{2l}\frac{\cos\beta - \cos[(2k+1)\beta]}{\cos(k\beta)} < 0. \end{aligned} \tag{33}$$

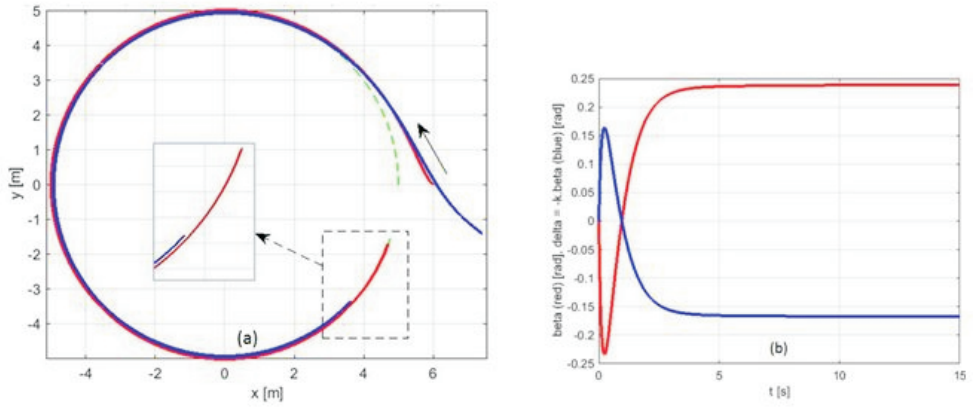

Fig. 2. (a) Following a circular path: The path drawn by the car reference point S (red line), the rear point P (blue line) and the point R of reference path (green dashed line); (b) Evolution in time of the front steering angle $\beta(t)$ (red line) and rear steering angle $\delta = -k\beta$ (blue line)

Since $\cos\beta - \cos[(2k+1)\beta] > 0$ for $k > 0$, the derivative of V is negative definite for $k > 0$. Hence, the zero dynamics is asymptotically stable. This completes the proof. □

Therefore, the proposed feedback control stabilizes the overall third-order system.

4. Simulation results. Simulation results were performed to verify the functionality and illustrate the effectiveness of the proposed path following controller. The algorithm developed in Section 3 was implemented in MATLAB. A circular reference path with radius $\rho_r = 5$ m was chosen for the simulations. The wheel base of the car was chosen to be $l = 2$ m, and the rear-to-front steering angle ratio $k = 0.7$. The controller parameters were specified as $k_1 = 4$, $k_2 = 0.2$. The time-varying linear car velocity was set to be $v = 2 + \sin(0.8 * t)$ m/s. The initial conditions for the tracking errors were set to be $y_e(0) = -1$ m, $\varphi_{\beta e}(0) = \pi/4$ rad and $\beta(0) = 0$ rad.

Simulation results of the planar car path in the $x-y$ plane traced by the front reference point S (red line), as well as rear point P (blue line) and point R associates with the reference path (green dashed line), are shown in Fig. 2a. It can be seen that the path drawn from the front axle centre point S (red line), which is the reference point of the bi-steerable car, asymptotically approaches the reference circular path (green dashed line), and it takes about 5 s before the reference path is successfully tracked. The trajectory of the rear centre point P (blue line) in steady-state is similar to those of point S. The smaller turning radius of 4.93 m or 0.07 m difference compared to the turning radius of 5 m of the front axle centre point S, is due to the fact that rear-to-front steering angle ratio $k = 0.7$ is smaller than 1. It is to note that, in the case of symmetric steering

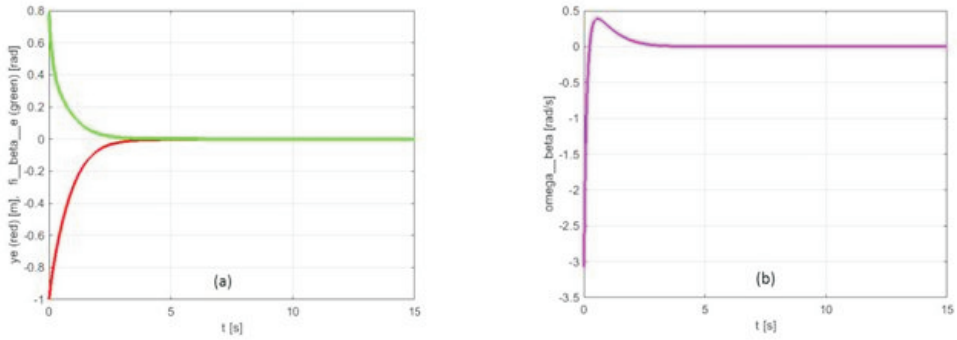

Fig. 3. (a) Evolution in time of the error coordinates: the lateral error $y_e(t)$ (red line) and orientation error $\varphi_{\beta e}(0)$ (green line); (b) Evolution of time of the control input $\omega(t)$ (steering angular velocity) of the front steering wheel

$\beta = -\delta$ $(k = 1)$, during the vehicle motion along a circular reference path, at steady-state, the rear centre axle point P will follow exactly the same path of the reference front axle centre point S, i.e., the two points will draw concentric arcs of circles of same radii. Therefore, when using front and rear wheel steering, the turning capabilities of the car are improved considerably The evolution of the front and rear steering angles β (red line) and the rear steering angle $\delta = -0.7\beta$ (blue line) with respect to time t, are presented in Fig. 2b. At steady-state, the front wheel steering angle β is approximately 0.238 rad (13.6 deg), whereas the rear wheel steering angle δ is equal to -0.167 rad (-9.5 deg). From the simulation, it can be seen that front wheel steering angle, (as well as the rear wheel steering angle) is bounded and asymptotically converges to finite value, when the car reaches the circular reference path, which confirm that the zero dynamics of the system is asymptotically stable, and this is in conformity with Proposition 2 in Section 3. The evolution of the lateral and orientation error coordinates $y_e(t)$ (red line) and $\varphi_{\beta e}(t)$ (green line) with respect to time t, are given in Fig. 3a. It can be seen that the tracking errors converge asymptotically to zero, which is in conformity with Proposition 1 in Section 3. Time-domain variation of the control input $\omega(t)$ (steering angular velocity) of the front steering angle, is shown in Fig. 3b. It can be observed that the control is bounded and after approximately 5 s its value approaches zero, since the automated car tracks a circular reference path. Simulation results demonstrate the ability of the controller to follow precisely a curvilinear reference with time-varying vehicle velocity. They also confirm the validity of the proposed control design approach based on a reduced-order model and the theoretical results obtained in the previous Section, that the proposed controller successfully stabilizes the entire third order system.

5. Conclusion. This paper presents a path following controller for a bi-steerable car. The path tracking controller addresses the need of the autonomous

bi-steerable vehicle to precisely follow a given path with various radius of curvature and with time-varying vehicle velocity. The proposed controller relies on a developed kinematic model of a nonholonomic bi-steerable car using a single track model. The path following error kinematics is derived with respect to the lateral position error and orientation error with respect to the reference path, which are used as indexes for performance evaluation of the designed controller. The path following problem is solved by a control, which is designed via Lyapunov techniques, and asymptotic path tracking convergence is proved. Moreover, a stability property of the internal dynamics is established, showing that asymptotic stability of the overall closed-loop system is preserved. Simulations are carried out which show the effectiveness of the proposed controller to achieve a good tracking accuracy. The results from the simulation tests also show the benefit of rear wheel steering which can provide enhanced manoeuvrability during manoeuvres in confined spaces at lower speed, and which is important for accurate path following in clutter environments.

REFERENCES

[1] Li L., J. Li, S. Zhang (2021) Review article: State-of-the-art trajectory tracking of autonomous vehicles, Mech. Science, **12**, 419–432.

[2] Jacob S., L. Varghese, J. Selvaraj, S. Shanmugam (2024) Machine learning assisted autonomous vehicle in an IoT environment, C. R. Acad. Bulg. Sci., **77**(3), 399–407.

[3] Pleshkova S. (2023) Self-driving car control model extension with voice commands control, C. R. Acad. Bulg. Sci., **76**(11), 1743–1753.

[4] Manivel M., L. Kaliappan (2023) Design and implementation of modified multilevel inverter fed BLDC motor for electric vehicle application, C. R. Acad. Bulg. Sci., **76**(10), 1562–1571.

[5] Hung N., F. Rego, J. Quintas et al. (2022) A review of path following control strategies for autonomous robotic vehicles: Theory, simulations, and experiments, J. Field Robotics, **40**(3) 747–779.

[6] Hang P., X. Chen (2021) Towards autonomous driving: Review and perspectives on configuration and control of four-wheel independent drive/steering electric vehicles, Actuators, **10**(184), 1–21.

[7] Sekhavat S., J. Hermosillo (2002) Cycab bi-steerable cars: a new family of differentially flat systems, Adv. Robotics, **16**(5), 445–462.

[8] Hamerlain F., S. Tchenderli-Braham (2017) Reduction of chattering for a sliding mode control of a bi-steerable car, Proc. 11th Asian Control Conference, 606–611.

[9] Zhang C., G. Gao, C. Zhao et al. (2022) Research on 4WS agricultural machine path tracking, Machines, **10**(597), 1–21.

[10] Petrov P., I. Kralov (2023) Modelling and feedback control for reversing a nonholonomic mobile robot platoon, C. R. Acad. Bulg. Sci., **76**(9), 1402–1412.

[11] Petrov P., I. Kralov (2021) Adaptive formation control of nonholonomic mobile robots for autonomous following in front of the leader, C. R. Acad. Bulg. Sci., **74**(9), 1370–1379.
[12] Slotine J.-J. E., W. Li (1991) Applied Nonlinear Control, Prentice Hall, New Jersey.

[1]*Faculty of Mechanical Engineering, Technical University of Sofia,*
8 Kliment Ohridski Blvd, 1756 Sofia, Bulgaria
e-mail: ppetrov@tu-sofia.bg

[2]*Department of Mechanics, Technical University of Sofia,*
8 Kliment Ohridski Blvd, 1756 Sofia, Bulgaria
e-mail: kralov@tu-sofia.bg